

See discussions, stats, and author profiles for this publication at: <https://www.researchgate.net/publication/231667016>

Designing Lower Critical Solution Temperature Behavior into a Discotic Small Molecule

ARTICLE *in* JOURNAL OF PHYSICAL CHEMISTRY LETTERS · APRIL 2010

Impact Factor: 7.46 · DOI: 10.1021/jz100307y

CITATIONS

10

READS

49

5 AUTHORS, INCLUDING:



[Jan Labuta](#)

National Institute for Materials Science

30 PUBLICATIONS 376 CITATIONS

[SEE PROFILE](#)



[Jonathan P Hill](#)

National Institute for Materials Science

286 PUBLICATIONS 8,687 CITATIONS

[SEE PROFILE](#)



[Toshiyuki Mori](#)

National Institute for Materials Science

302 PUBLICATIONS 6,304 CITATIONS

[SEE PROFILE](#)



[Katsuhiko Ariga](#)

National Institute for Materials Science

623 PUBLICATIONS 21,615 CITATIONS

[SEE PROFILE](#)

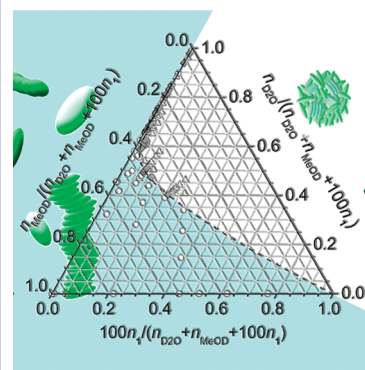
Designing Lower Critical Solution Temperature Behavior into a Discotic Small Molecule

Gary J. Richards,[†] Jan Labuta,[†] Jonathan P. Hill,^{*,†} Toshiyuki Mori,[†] and Katsuhiko Ariga[†]

[†]WPI Center for Materials Nanoarchitectonics (MANA), National Institute for Materials Science (NIMS), JST-CREST, Namiki 1-1, Tsukuba, Ibaraki 305-0044, Japan, and ^{*}Nanoionics Group, Fuel Cell Materials Group, National Institute for Materials Science, Namiki 1-1, Tsukuba, Ibaraki 305-0044, Japan

ABSTRACT Design and analysis of amphiphilic small molecules exhibiting lower critical solution temperature (LCST) behavior is reported. 2,3,6,7,10,11-Hexakis-[2-(*N,N*-dialkylamino)ethoxy] triphenylenes containing hydrophilic groups attached at their discotic core were prepared, and the LCST behavior of their solutions was studied using fluorescence spectrophotometry and ¹H NMR spectroscopy. ¹H NMR spin–lattice relaxation times were used to assess the rotational mobility of molecules below and above the clouding point. The impact on the LCST of supramolecular π – π stacking forces introduced by the triphenylene (TP) core was studied. The operation of the LCST phenomenon was found not to depend significantly on stacking of TP moieties. This process in small molecular species offers several advantages over the polymer-originated phenomenon. For instance, enabling an analogue of the LCST transition in dye molecules might allow the design of novel optical devices by permitting previously unavailable specific aggregated states.

SECTION Macromolecules, Soft Matter



A phase separation event in solutions of some polymers is characterized by a lower critical solution temperature (LCST)^{1,2} and is often referred to as the coil–globule (C–G) transition because of changes occurring in the structure of the polymer backbone.^{3–5} It is an entropy-driven process caused by variation in the interaction between the polymer and solvent molecules, especially through hydration at hydrophilic main-chain or side-group substituents, and it provides a means for using a bulk-scale phenomenon to control aggregated states at the molecular or nanoscales. The great significance of the LCST phenomenon lies in the fact that it occurs not only in man-made polymers such as poly(*N*-isopropylacrylamide) (PNIPAAm)^{6–8} and poly(vinyl methyl ether) (PVME)^{9,10} but also in biopolymers such as proteins, where it is a factor in denaturation. In most cases, high molecular weight species are involved, although it is known that some small molecules such as triethylamine^{11,12} and nicotine^{13,14} possess critical point behavior of their aqueous solutions.^{15,16} In addition, there have been recent reports involving LCST in a small molecule¹⁷ or dendrimers.¹⁸ In the former, prior self-assembly to an oligomeric aggregate precedes operation of the LCST effect.¹⁷ With these facts in mind, we postulated that a small molecule bearing similar (i.e., ternary alkylamine) substituents should also be capable of undergoing processes analogous to the LCST caused by changes in molecular solvation and aggregate structure if appropriate peripheral groups could be introduced. For this purpose, and for ease of synthesis, we elected to prepare hexa-substituted triphenylenes bearing triethylamine groups.

Triphenylenes¹⁹ **1** and **2** (Figure 1a) with peripheral triethylamine substituents linked through alkoxy linkages, both of which are known to promote the C–G transition,^{6–10,20,21} were prepared.²² These molecules have discotic tendencies,²³ as indicated by a mesophase observed for **2**.

Triphenylenes **1** and **2** both exhibit clouding of aqueous methanol solutions ($c = \sim 1$ mM, 40 % v/v H₂O/MeOH) with increasing temperature characteristic of LCST behavior. Cooling the solution stimulates the reverse process. A plot of the temperature dependency of the solution transmittance (Figure 1b) is accompanied by photographs of a solution below and above its clouding point. These observations, including the microscopic morphological change (Figure 1c), are qualitatively similar to those made at the C–G transition of polymers.^{24,25} Here, the mechanism of the process for **1** was studied by using fluorescence and ¹H NMR spectroscopy.

In triphenylenes, stacking through π – π interactions results in new red-shifted bands in their fluorescence spectra.²⁶ In solutions of **1** in dichloromethane, at low concentration ($c = 0.1$ mM), fluorescence spectrophotometry indicates that π – π interaction does not occur, although at higher concentrations ($c \geq 1.0$ mM), it becomes increasingly important (Figure 1d(i)). Fluorescence measurements on solutions of **1** in a H₂O/MeOH mixture (v/v % water in methanol $\phi_{\text{H}_2\text{O}} = 40$ % v/v) resulted in similar observations (Figure 1d(ii)).

Received Date: March 9, 2010

Accepted Date: April 6, 2010

Published on Web Date: April 09, 2010

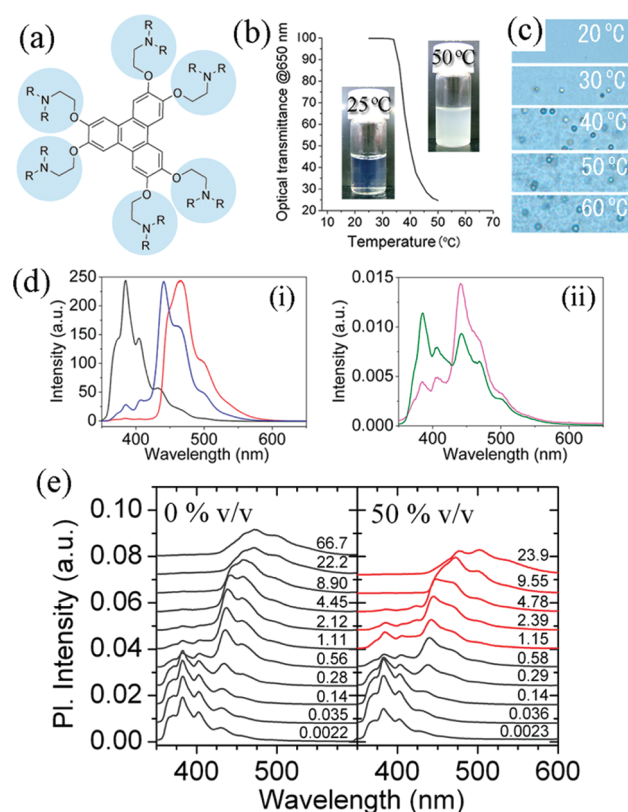


Figure 1. (a) Chemical structure of **1** ($R = \text{CH}_2\text{CH}_3$) and **2** ($R = \text{CH}_2\text{CH}=\text{CH}_2$). (b) Optical transmittance at 650 nm of a solution of **1** ($c \approx 1$ mM, $\text{H}_2\text{O}/\text{MeOH}$ ratio $\phi_{\text{H}_2\text{O}} = 40\%$ v/v) accompanied by photographs above and below its clouding point. (c) Optical micrographs ($\times 20$) of a solution of **1** ($c \approx 1$ mM, $\phi_{\text{H}_2\text{O}} = 40\%$ v/v) upon heating from 20 to 60 °C. (d) Normalized fluorescence spectra of **1** (i) in CH_2Cl_2 at 20 °C and $c = 0.1$ mM (black line, not stacked), 1.0 mM (blue, partially stacked), and 10 mM (red, stacking occurs) and (ii) in $\text{H}_2\text{O}/\text{MeOH}$ ($\phi_{\text{H}_2\text{O}} = 40\%$ v/v; $c = 1.2$ mM) below (20 °C mauve line,) and above (50 °C, green) the LCST. (e) Normalized fluorescence spectra of **1** in the range of c from ~ 67 to 0.002 mM (noted at each curve) at 20 °C measured for two solvent compositions $\phi_{\text{H}_2\text{O}} = 0$ and 50% v/v. Red lines denote phase separation as indicated by solution opacity.

However, there is a significant difference between solutions of **1** in dichloromethane and its solutions in aqueous solvent mixtures in that warming of the latter above a certain temperature (which can be close to ambient temperature depending on solvent composition $\phi_{\text{H}_2\text{O}}$) results in clouding (Figure 1b,c).

To understand the mechanism of the clouding process in $\text{H}_2\text{O}/\text{MeOH}$ mixtures, we studied the temperature dependency of fluorescence emission spectra of solutions of **1** in $\text{H}_2\text{O}/\text{MeOH}$ mixtures. At temperatures below the clouding point and at high concentrations (above 1 mM), the triphenylene molecules are stacked through π – π interactions,²⁷ and in the case of **1**, these stacks possess multiple hydrophilic amine and alkoxy side groups as potential solvent hydrogen bonding sites. Upon heating above the clouding point, fluorescence emission due to π – π stacking is somewhat reduced, indicating a partial disruption of this interaction in the high-temperature phase (Figure 1d(ii)).²⁶ This is counterintuitive given the expected preference of the triphenylene moiety to undergo

stacking interactions.^{28–30} In order to determine the dependence of stacking interactions on the concentration c of **1**, spectra were collected over a broad range of concentrations for two $\text{H}_2\text{O}/\text{MeOH}$ mixtures ($\phi_{\text{H}_2\text{O}} = 0$ and 50% v/v) at 20 °C (Figure 1e). Fluorescence spectra are similar for both solvent compositions, although at $\phi_{\text{H}_2\text{O}} = 50\%$ v/v, solutions with $c \geq 1.15$ mM exhibit a phase separation (red lines, Figure 1e). Fluorescence spectra in the two different solvent mixtures (and with varying concentrations²²) indicate that in solutions where the LCST can occur, the only significant concomitant change in the fluorescence spectrum that was observed was an increase in fluorescence due to nonstacked **1**. In fact, some variation in fluorescence spectra can be observed at the LCST only in solutions where stacking should be occurring (as indicated by fluorescence spectra). Therefore, (a) LCST occurs even when stacking of **1** appears minimal; (b) when stacking can be detected in the fluorescence spectrum, it is always apparently partially disrupted upon LCST.

¹H NMR T_1 spin–lattice relaxation times in solutions of **1** (in $\text{D}_2\text{O}/\text{methanol-}d_4$) above and below the clouding point²² clearly indicate that **1** is more highly aggregated above the clouding point despite the reduction in π – π stacking apparent from fluorescence emission measurements (Figure 1d(ii)). Typical changes in the ¹H NMR spectra caused by the LCST event are shown in Figure 2a, revealing new sets of peaks at higher field (marked red) due to the phase separation process. ¹H NMR spectra were collected for a wide range of concentrations of **1** and compositions of the solvent mixtures at low (15 °C) and high (50 °C) temperature with three types of behavior being observed (homogeneous, reversible dissolution–aggregation, and/or opaque), which are respectively represented by the NMR spectra shown in Figure 2b(i), (ii), and (iii). These data were used to construct a phase diagram of the clouding process (Figure 3a). A clearly demarcated boundary region emerged between the homogeneous solution state and the opaque state. Solutions of composition close to this boundary undergo a fully reversible critical solution process between 15 and 50 °C. Here, the phase separation induced by increasing temperature leads to differences in the internal structure of the aggregates depending on the location at the boundary region. At high concentrations (above 1 mM), the solution-state stacked structure of **1** is, to some degree, broken upon clouding. However, π – π stacking is still evident but less favored inside of these aggregates because of increased competition from intermolecular hydrogen bonding (which obstructs π – π stacking) and due to increased hydrophobicity at the interior of the aggregates (due to lower solvent content relative to the surrounding medium, which undermines amphiphilicity of **1**). Conversely, in low-concentration solutions, π – π stacking hardly occurs below or above the clouding point. These observations indicate that the LCST behavior of **1** is more strongly dependent on the nature of its peripheral groups rather than the stacking tendencies of the triphenylene moieties. Although the stacking forces in triphenylenes are often considered strong, in this case, their effect is less important due to their relatively short range of effectiveness when compared with hydrogen bonding interactions, which are thought to dominate in this kind of aggregation process.³¹ Our observations can be summarized as the model shown in

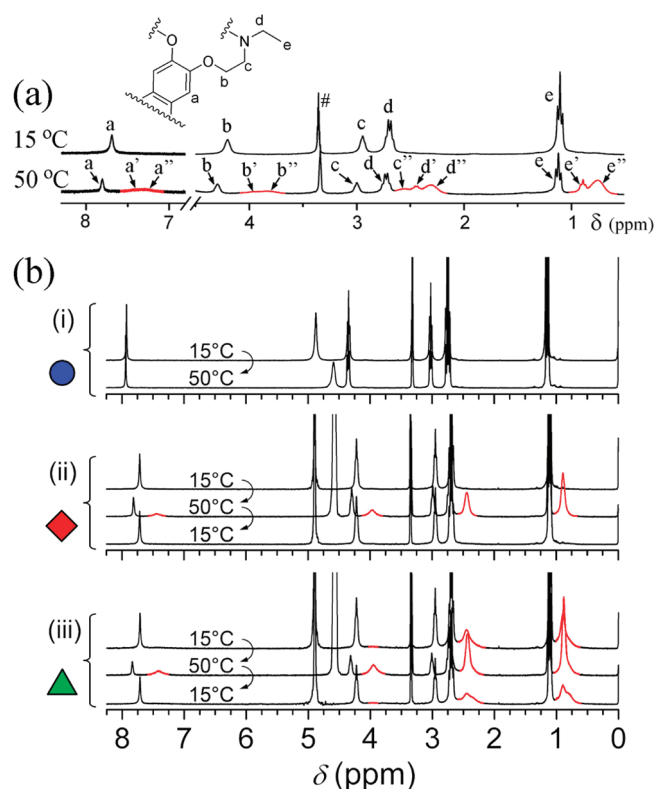


Figure 2. (a) ^1H NMR spectra of **1** in D_2O /methanol- d_4 below ($15\text{ }^\circ\text{C}$) and above ($50\text{ }^\circ\text{C}$) the LCST ($c \approx 1\text{ mM}$, $\phi_{\text{D}_2\text{O}} = 40\%\text{ v/v}$). Assignments (see partial structure) are given in the spectra. Peaks due to phase-separated **1** (marked red) are labeled single prime and double prime. # denotes the peak due to methanol. (b) Typical VT- ^1H NMR measurements used for construction of the phase diagram. Three types of phase behavior due to **1**: (i) (blue circle) homogeneous state (no aggregation even at $50\text{ }^\circ\text{C}$); (ii) (red diamond) boundary region (reversible dissolution–aggregation process between 50 and $15\text{ }^\circ\text{C}$); (iii) (green triangle) opaque (aggregates always present even at $15\text{ }^\circ\text{C}$).

Figure 3b. Other characteristics of the LCST process for **1**, such as the dependence of percentage fractions of phase-separated molecules on solvent composition ($\phi_{\text{D}_2\text{O}}$), could also be determined from VT- ^1H NMR spectra (Figure 4). These data also show that with increasing $\phi_{\text{D}_2\text{O}}$ (increased proportion of D_2O in the solvent mixture), the critical temperature is depressed and that there is a clear hysteresis in the LCST process of **1** because the rate of dissolution is slower than the rate for aggregative precipitation (Figure 4b).

In conclusion, we have designed a means for introducing critical temperature behavior to triphenylene molecules, and we have analyzed the process from the point of view of the molecules' solvation and aggregation properties. Our results indicate that the LCST phenomenon in small molecules offers unexpected states of aggregation that might be important in optical applications and that this macroscale effect allows control of the chromophores' structure at the molecular scale. Also, we expect that our design protocol of introducing LCST-promoting groups into small molecules will ultimately result in the observation of this phenomenon in a greater variety of molecular chromophores, and we are currently working toward this.

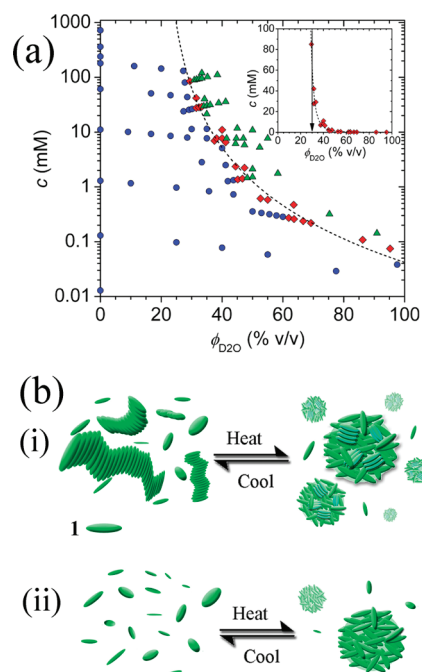


Figure 3. (a) Concentration (c)–composition ($\phi_{\text{D}_2\text{O}}$) phase diagram from ^1H NMR measurements. Three types of behavior are denoted as (blue circles) homogeneous (no aggregation even at $50\text{ }^\circ\text{C}$); (red diamonds) boundary region (reversible dissolution–aggregation process between 50 and $15\text{ }^\circ\text{C}$); (green triangles) opaque (aggregates always present even at $15\text{ }^\circ\text{C}$). The inset shows the boundary region in a c -linear scale chart. (b) Model of the aggregation processes involved in the critical solution temperature behavior, (i) high concentration behavior ($c \geq 1.0\text{ mM}$) and (ii) low concentration behavior ($c \leq 0.1\text{ mM}$).

EXPERIMENTAL METHODS

Hexakis(2-(*N,N*-diethylamino)ethoxy)triphenylene, 1. A mixture of hexakis(2-(4-toluenesulfonyl) ethyloxy)triphenylene (200 mg , $1.32 \times 10^{-4}\text{ mol}$), diethylamine (0.77 g , $1.06 \times 10^{-2}\text{ mol}$), and sodium carbonate (150 mg , $1.42 \times 10^{-3}\text{ mol}$) in acetonitrile (10 mL) was heated at reflux for 24 h . The mixture was allowed to cool, and water (50 mL) was added; then, the mixture was extracted with dichloromethane ($2 \times 25\text{ mL}$). The dichloromethane extracts were combined, dried over anhydrous Na_2SO_4 , filtered, and concentrated, giving an orange solid. The crude product was dissolved in methanol and precipitated in water to give a yellow solid, which was filtered and dried under reduced pressure. The product was further purified by column chromatography (basic alumina, eluent 10% methanol in dichloromethane) to give the title product as a yellow solid. Yield: 67 mg (55%). MP: $80\text{ }^\circ\text{C}$. FTIR (KBr pellet): 2931 , 2803 (CH stretch); 1617 (C=C stretch), 1519 (C=C stretch), 1439 (CH_2 def), 1383 , 1263 , 1177 , 1050 (C–N stretch), 840 (C–H bend) cm^{-1} . ^1H NMR (CDCl_3 , $20\text{ }^\circ\text{C}$, 300 MHz): $\delta = 7.85$ (s, 6H , ArH), 4.32 (t, 12H , ArOCH_2 , $J = 6.33\text{ Hz}$), 3.05 (t, 12H , $\text{ArOCH}_2\text{CH}_2$, $J = 6.36\text{ Hz}$), 2.74 (quart, 24H , NCH_2CH_3 , $J = 7.05\text{ Hz}$), 1.13 (t, 36H , NCH_2CH_3 , $J = 7.05\text{ Hz}$) ppm. ^{13}C NMR (CDCl_3 , $20\text{ }^\circ\text{C}$, 75 MHz): $\delta = 148.50$, 123.53 , 106.59 , 67.84 , 51.79 , 47.90 , 11.93 ppm. MALDI-TOF-MS (dithranol): calculated for $\text{C}_{54}\text{H}_{90}\text{N}_6\text{O}_6$, $m/z = 918.69$; found, 919 [M]^+ .

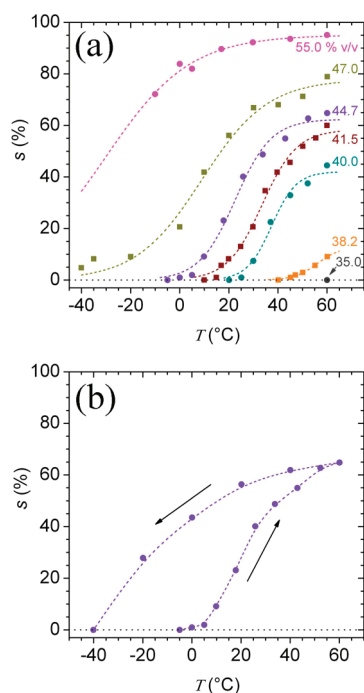


Figure 4. (a) Percentage fraction of phase-separated moieties s as determined from VT- ^1H NMR measurements (data for CH_3 resonance of **1** are presented) using the formula given below. The figure illustrates temperature dependences of samples with a constant concentration of **1** ($c = 7.69$ mM) and various solvent compositions (ϕ_{D_2O} is indicated at each curve). (b) Reversible procedure showing hysteresis in the dissolution–aggregation process as measured on a sample with $c = 7.69$ mM and $\phi_{D_2O} = 44.7\%$ v/v. Arrows indicate the direction upon heating (\rightarrow) and cooling (\leftarrow). Data were collected after equilibrating at each temperature for 60 s. Formula: $s = [I_{\text{separated}} / (I_{\text{nonseparated}} + I_{\text{separated}})] \times 100\%$, where $I_{\text{separated}}$ is the integrated intensity of the terminal CH_3 resonance (see protons labeled (e'), e'') in Figure 2a), corresponding to the new peaks at higher field due to temperature-induced aggregation of **1**, and $I_{\text{nonseparated}}$ is the integrated intensity of the terminal CH_3 (protons labeled (e)) in the original nonaggregated state.

^1H NMR Spectroscopy. ^1H NMR spectra were collected using a JEOL AL300BX spectrometer operating at 300.4 MHz. Variable-temperature measurements (VT- ^1H NMR) were performed using the appropriate JEOL temperature control unit (temperature fluctuation, ± 0.3 °C).

SUPPORTING INFORMATION AVAILABLE Synthetic details and additional characterization including further fluorescence and ^1H NMR data. This material is available free of charge via the Internet at <http://pubs.acs.org>.

AUTHOR INFORMATION

Corresponding Author:

*To whom correspondence should be addressed. E-mail: Jonathan.Hill@nims.go.jp.

ACKNOWLEDGMENT This research was supported by the World Premier International Research Center Initiative (WPI Initiative) on Materials Nanoarchitectonics from Ministry of Education, Culture,

Sports, Science and Technology (MEXT), Japan, and by JST, CREST, and Japan Society for the Promotion of Science (JSPS) in the form of a fellowship to J.L.

REFERENCES

- (1) Stockmayer, W. H. Forces between Macromolecules. *Rev. Mod. Phys.* **1959**, *31*, 103–106.
- (2) Tanaka, T. Collapse of Gels and Critical Endpoint. *Phys. Rev. Lett.* **1978**, *40*, 820–823.
- (3) Urry, D. W. Physical Chemistry of Biological Free Energy Transduction as Demonstrated by Elastic Protein-Based Polymers. *J. Phys. Chem. B* **1997**, *101*, 11007–11028.
- (4) Sun, S. T.; Nishio, I.; Swislow, G.; Tanaka, T. The Coil–Globule Transition — Radius of Gyration of Polystyrene in Cyclohexane. *J. Chem. Phys.* **1980**, *73*, 5971–5975.
- (5) Molyneux, P. *Water-Soluble Synthetic Polymers: Properties and Behavior*; CRC Press: Boca Raton, FL, 1983; Vol. 1, pp 58–61.
- (6) Heskins, M.; Guillet, J. E.; James, E. Solution Properties of Poly(N-isopropylacrylamide). *J. Macromol. Sci., Chem.* **1968**, *A2*, 1441–1455.
- (7) Schild, H. G. Poly(N-isopropylacrylamide) — Experiment, Theory and Application. *Prog. Polym. Sci.* **1992**, *17*, 163–249.
- (8) Chen, G.; Hoffman, A. S. Graft Copolymers that Exhibit Temperature-Induced Phase Transitions Over a Wide Range of pH. *Nature* **1995**, *373*, 49–52.
- (9) Maeda, H. Interaction of Water with Poly(vinyl methyl-ether) in Aqueous Solution. *J. Polym. Sci., Part B: Polym. Phys.* **1994**, *32*, 91–97.
- (10) Hanyková, L.; Labuta, J.; Spěváček, J. Effect of Time on the Hydration and Temperature-Induced Phase Separation in Aqueous Polymer Solutions. ^1H NMR Study. *Polymer* **2006**, *47*, 6107–6116.
- (11) Kohler, F.; Rice, O. K. Coexistence Curve of the Triethylamine–Water System. *J. Chem. Phys.* **1957**, *26*, 1614–1618.
- (12) Flewelling, A. C.; DeFonseka, R. J.; Khaleeli, N.; Partee, J.; Jacobs, D. T. Heat Capacity Anomaly near the Lower Critical Consolute Point of Triethylamine–Water. *J. Chem. Phys.* **1996**, *104*, 8048–8057.
- (13) Davies, N. S. A.; Gillard, R. D. The Solubility Loop of Nicotine Water. *Trans. Met. Chem.* **2000**, *25*, 628–629.
- (14) Ladd, M. *Introduction to Physical Chemistry*; Cambridge University Press: Cambridge, U.K., 1998; pp 316–319.
- (15) Hirose, T.; Matsuda, K.; Irie, M. Self-Assembly of Photochrome Diarylethenes with Amphiphilic Side Chains: Reversible Thermal and Photochemical Control. *J. Org. Chem.* **2006**, *71*, 7499–7508.
- (16) Hirose, T.; Matsuda, K.; Irie, M. Temperature-Light Dual Control of Clouding Behavior of an Oligo(ethylene glycol)–Diarylethene Hybrid System. *Adv. Mater.* **2008**, *20*, 2137–2141.
- (17) Betancourt, J. E.; Rivera, J. M. Nonpolymeric Thermosensitive Supramolecules. *J. Am. Chem. Soc.* **2009**, *131*, 16666–16668.
- (18) Aathimanikandan, S. V.; Savariar, E. N.; Thayumanavan, S. Temperature-Sensitive Dendritic Micelles. *J. Am. Chem. Soc.* **2005**, *127*, 14922–14929.
- (19) Ahmed, F. R.; Trotter, J. Crystal Structure of Triphenylene. *Acta Crystallogr.* **1963**, *16*, 503–508.
- (20) Van Durme, K.; Van Mele, B.; Bernaerts, K. V.; Verdonck, B.; Du Prez, F. E. End-Group Modified Poly(methyl vinyl ether): Characterization and LCST Demixing Behavior in Water. *J. Polymer Sci., Part B: Polym. Phys.* **2006**, *44*, 461–469.
- (21) Aseyev, V.; Hietala, S.; Laukkanen, A.; Nuopponen, M.; Confortini, O.; Du Prez, F. E.; Tenhu, H. Mesoglobules of

Thermoresponsive Polymers in Dilute Aqueous Solutions above the LCST. *Polymer* **2005**, *46*, 7118–7131.

- (22) See Supporting Information.
- (23) Cammidge, A. N.; Bushby, R. J. In *Handbook of Liquid Crystals*; Demus, D., Goodby, J. W., Gray, G. W., Spiess, H. W., Vill, V., Eds.; Wiley VCH: New York, 1998; Vol. 2B, pp 693–748.
- (24) Tanaka, H.; Nishi, T. Initial Stage of Separation in a Binary Mixture of Poly(vinyl methyl ether) and Water. *Jpn. J. Appl. Phys.* **1988**, *27*, 1783–1786.
- (25) Tanaka, H. Unusual Phase Separation in a Polymer Solution caused by Asymmetric Molecular Dynamics. *Phys. Rev. Lett.* **1993**, *71*, 3158–3161.
- (26) Ikeda, M.; Takeuchi, M.; Shinkai, S. Unusual Emission Properties of a Triphenylene-Based Organogel System. *Chem. Commun.* **2003**, 1354–1355.
- (27) The lack of a broad excimer-type emission band at around 540 nm indicates that stacking is through either staggered or slipped stack modes and does not involve full eclipse of the triphenylene moieties (see ref 26).
- (28) Destrade, C.; Tinh, N. H.; Malthete, J.; Levelut, A. M. On the Rectangular-Hexagonal Columnar Phase Transition in Disk-Like Liquid Crystals. *J. Phys. (Paris)* **1983**, *44*, 597–602.
- (29) Heiney, P. A.; Fontes, E.; de Jeu, W. H.; Riera, A.; Carroll, P.; Smith, A. B. Frustration and Helicity in the Ordered Phases of a Discotic Compound. *J. Phys. (Paris)* **1989**, *50*, 461–483.
- (30) Boden, N.; Bushby, R. J.; Lozman, O. R. Designing Better Columnar Mesophases. *Mol. Cryst. Liq. Cryst.* **2003**, *400*, 105–113.
- (31) Chandler, D. Interfaces and the Driving Force of Hydrophobic Assembly. *Nature* **2005**, *437*, 640–647.